Journal of Hazardous Materials 161 (2009) 854–861

Contents lists available at ScienceDirect

Journal of Hazardous Materials

journal homepage: www.elsevier.com/locate/jhazmat

Cesium adsorption and distribution onto crushed granite under different physicochemical conditions

Shih-Chin Tsai[a], Tsing-Hai Wang[b], Ming-Hsu Li[c], Yuan-Yaw Wei[a], Shi-Ping Teng[b,d,*]

[a] Nuclear Science and Technology Development Center, National Tsing Hua University, Hsinchu 300, Taiwan, ROC
[b] Institute of Nuclear Engineering and Science, National Tsing Hua University, Hsinchu 300, Taiwan, ROC
[c] Institute of Hydrological Sciences, National Central University, Jungli 320, Taiwan, ROC
[d] Department of Engineering and System Science, National Tsing Hua University, Hsinchu 300, Taiwan, ROC

ARTICLE INFO

Article history:
Received 27 January 2007
Received in revised form 8 April 2008
Accepted 13 April 2008
Available online 20 April 2008

Keywords:
Granite
Cesium
Kinetic
Isotherm
Thermodynamic
Surface distribution

ABSTRACT

The adsorption of cesium onto crushed granite was investigated under different physicochemical conditions including contact time, Cs loading, ionic strength and temperature. In addition, the distribution of adsorbed Cs was examined by X-ray diffraction (XRD) and EDS mapping techniques. The results showed that Cs adsorption to crushed granite behaved as a first-order reaction with nice regression coefficients ($R^2 \geqq 0.971$). Both Freundlich and Langmuir models were applicable to describe the adsorption. The maximum sorption capacity determined by Langmuir model was 80 μmol g^{-1} at 25 °C and 10 μmol g^{-1} at 55 °C. The reduced sorption capacity at high temperature was related to the partial enhancement of desorption from granite surface. In general, Cs adsorption was exothermic ($\Delta H < 0$, with median of -12 kJ mol^{-1}) and spontaneous ($\Delta G < 0$, with median of -6.1 at 25 °C and -5.0 kJ mol^{-1} at 55 °C). The presence of competing cations such as sodium and potassium ions in synthetic groundwater significantly reduces the Cs adsorption onto granite. The scanning electron microscopy–energy dispersive X-ray spectroscopy (SEM/EDS) mapping method provided substantial evidences that micaceous minerals (biotite in this case) dominate Cs adsorption. These adsorbed Cs ions were notably distributed onto the frayed edges of biotite minerals. More importantly, the locations of these adsorbed Cs were coincided with the potassium depletion area, implying the displacement of K by Cs adsorption. Further XRD patterns displayed a decreased intensity of signal of biotite as the Cs loading increased, revealing that the interlayer space of biotite was affected by Cs adsorption.

1. Introduction

Nuclear power is one of the reliable and abundant power sources with an attractive advantage of zero carbon dioxide emission. However, the safety of spent nuclear fuel is of concern to the general public because it requires thousands year's of disposal. To reduce the possibility of the release of these radionuclides into environment, the design of a multilayer repository is adopted. The selection of buffer/backfill materials and geochemical host rock of the repository site should provide a high affinity environment to tightly retard the released radionuclides. The principal concept behind such design is to immobilize these released radionuclides via their adsorption or precipitation in buffer/backfill materials. Accordingly, a better understanding of the physicochemical behavior of radionuclides under possible geological environments is important to an accurate evaluation of the fate of these radionuclides. Although the geochemical conditions of waste repository sites might vary significantly even within meters, the laboratory scale investigation is still informative to quantify some transport-related parameters, i.e. K_d, distribution coefficient, for further hydrochemical transport simulations [1,2].

Among the radionuclides of concern, ^{137}Cs is an indicative nuclide because it is a high yield fission product and is a strong γ emitter. Together with its half-life of 30 years and high mobility in aqueous media, the migration of ^{137}Cs becomes a key criterion of performance assessment of radioactive waste repository. The mobility of these Cs radionculides can be considerably reduced by transferring them from aqueous phase onto rocks and minerals surface by an ion-exchange reaction [3–5]. In this work, granite is the rock of interest since it is a potential host rock for radioactive waste repository in Taiwan. Granite is a kind of igneous rock with advantages of abundance, toughness, and low porosity,

* Corresponding author at: Institute of Nuclear Engineering and Science, and Department of Engineering and System Science, National Tsing Hua University, Hsinchu 300, Taiwan, ROC. Tel.: +886 3 5742670; fax: +886 3 5720724.
E-mail address: spteng@ess.nthu.edu.tw (S.-P. Teng).

0304-3894/$ – see front matter © 2008 Elsevier B.V. All rights reserved.
doi:10.1016/j.jhazmat.2008.04.044

which is especially beneficial to the reduction of the migration of released radionuclides. In this report, a series of batch experiments is conducted to investigate the Cs adsorption onto granite under different physicochemical conditions including contact time, loadings of aqueous Cs ions, different ionic strength and reaction temperature. In addition, techniques of X-ray diffraction (XRD) and scanning electron microscopy–energy dispersive X-ray spectroscopy (SEM–EDS) are also utilized to examine the distribution of adsorbed Cs onto granite surface.

2. Materials and methods

2.1. Solid and liquid phases and chemicals

Granite rock samples were originated from Taiwan local area. The crushed granite samples were sieved and washed with ultrapure deionized water (DW, 18 MΩ, Milli-Q) to remove fine particles. The granite sands were stored in an oven at 60 °C under a reduced pressure to minimize the probability of any further phase transformation. The major constituent minerals were quartz, albite, biotite and goethite. The predominant elements, identified by ICP-MS (Sciex Elan 5000, PerkinElmer), presented as oxides were SiO_2 (72.56%), Al_2O_3 (12.9%), K_2O (8.84%), Na_2O (4.20%) and Fe_2O_3 (1.13%). The particle size of crushed granite samples used in this work was about 0.250–0.180 mm. The composition of synthetic groundwater (GW) and of synthetic seawater (SW) are shown in Table 1.

2.2. Batch experiments

The adsorption experiments were performed within serum bottles at two distinct temperatures of 25 °C and 55 °C, respectively. To investigate the characteristic of cesium adsorption to granite, 15 g of granite was immersed in 450 mL of $CsNO_3$ solution with concentration in the range of 1×10^{-3} M to 1×10^{-7} M, spiking with an appropriate amount of radioactive Cs-137 tracer. The utilization of 15 g of crushed granite was to reduce the influences from complex matrix of granite. The mixtures were then transferred into a water bath shaker equipped with a temperature controller. These Cs solutions were collected in the time period of 10 min, 30 min, 1 h, 2 h, 4 h, 8 h, 24 h, 48 h, 4 d and 7 d, respectively. During each sampling, 1 mL of the suspension was collected, filtrated through a 0.45 μm Millipore filter cell. Then, the radioactivity of these suspensions was counted with a NaI(Tl) detector (Wallac 1470 Wizard). After measurement, the suspension was immediately put back into the mixture to prevent any alterations of experimental conditions. The decrease of the radioactivity in these suspensions was deemed as the amount of adsorbed Cs ions on granite. At the same time, a parallel experiment without spiking radioactive tracer was conducted at 25 °C in order to collect further XRD and SEM/EDS information. To study the effect of ionic strength, a series of batch experiments was conducted with Cs loading of 1×10^{-4} M at 25 °C. The concentration of background electrolyte of four individual cations (Na^+, K^+, Ca^{2+} and Mg^{2+}) was in the range from 1.0 M to 1.0×10^{-3} M. In addition, Cs adsorption in synthetic groundwater and in synthetic seawater was also conducted to simulate the Cs adsorption behaviors in the real environment. These samples were continuously shaking for a week and the suspensions were collected following the aforementioned procedures.

Table 1
The composition of synthetic groundwater (GW) pH ~7.12, and of seawater (SW) pH ~7.32 used in this study

	GW (mol L^{-1})	SW (mol L^{-1})
Cl^-	1.78×10^{-1}	5.50×10^{-1}
Br^-	5.01×10^{-4}	8.39×10^{-4}
F^-	8.00×10^{-5}	6.80×10^{-5}
HCO_3^-	1.64×10^{-4}	–
SO_4^{2-}	5.83×10^{-3}	2.81×10^{-2}
BO_3^{3-}	–	4.16×10^{-4}
Na^+	9.13×10^{-2}	4.70×10^{-1}
K^+	2.07×10^{-4}	1.02×10^{-2}
Li^+	1.44×10^{-4}	2.50×10^{-5}
Ca^{2+}	4.72×10^{-2}	1.03×10^{-2}
Mg^{2+}	1.73×10^{-3}	5.31×10^{-2}
Sr^{2+}	4.00×10^{-4}	8.70×10^{-5}

2.3. Surface distribution of adsorbed Cs

To study the microscale distribution of adsorbed Cs ions, the granite sands were analyzed before and after Cs adsorption by XRD technique (Philips PW1300) and scanning electron microscopes equipped with energy dispersive X-ray spectroscope (SEM/EDS, Leo 1530). The XRD spectra were recorded in the range of 5–50° (2θ) by Cu Kα radiation (λ = 1.5406 Å) at 40 kV and 40 mA. The step size was 0.020 with a time duration of 60 s per step. The SEM/EDS was used to visualize the changes of adsorbed Cs on granite surface. The granite samples were adhered onto a conductive carbon taps on metallic disks. The EDS mappings were carried out at a voltage of 15 kV under vacuum condition and images of granite surface along with EDS mappings were recorded to study the sorption sites.

3. Results and discussion

3.1. Kinetic analysis

The kinetic adsorption experiments were conducted with five initial Cs concentrations ranging from 1×10^{-3} M to 1×10^{-7} M at two distinct temperatures of 25 and 55 °C. The variations of Cs concentration in solutions along with contact time were plotted in Fig. 1a (25 °C) and b (55 °C). It is observed that Cs adsorptions are instantaneous at given concentration range and the equilibria are reached within 8 h. This fast equilibrium is a typical adsorption feature of Cs onto minerals such as biotite, illite, hornblende, calcite and montmorillonite. It is noticed that this phenomenon is related to the adsorption taking place at the accessible sorption sites on external surface of these minerals [3,5] (Fig. 2).

For a better description of the kinetics of Cs adsorption, all the experimental data were fitted by a built-in first-order equation within Origin 6.0 Profession program (Microcal Software, USA) and expressed as the following:

$$[Cs]_l = a + b\,e^{-kt} \quad (1)$$

where $[Cs]_l$ is the aqueous concentration of Cs ions at time t (mol L^{-1}), a and b are constant (mol L^{-1}) and k is the first-order rate constant (h^{-1}). All the fitting results were listed in Table 2.

All R^2 values shown in Table 2 were close to unity, indicating that the Cs adsorption data was well fitted by the first-order equation. Accordingly, it is recognized that the Cs adsorption has a straightforward correlation with the Cs loading, which is consistent with the general description of Cs adsorption as the following:

$$\equiv ST_i - K + Cs^+ \leftrightarrow \equiv ST_i - Cs + K^+$$

where $\equiv ST_i$ stands for the ion-exchangeable site on granite surface, K is the potassium ion representing the exchangeable cation on micaceous minerals surface, i.e. biotite in this case [2].

With the help of kinetic fitting, it is observed that the rate constant, k, increases as Cs loading increases, implying that a slower

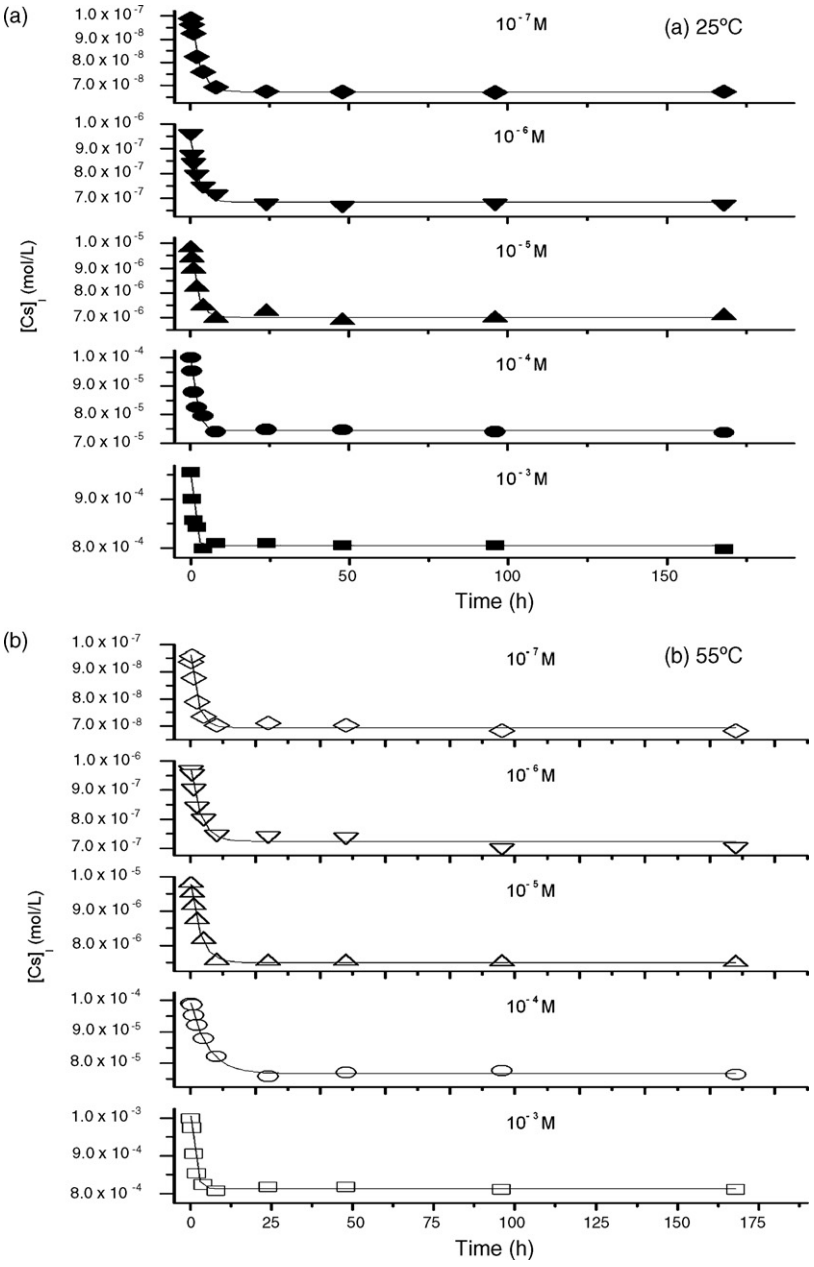

Fig. 1. Variation of remaining amount of Cs (M) in solution with reaction time. (a) At low temperature (25 °C); (b) at high temperature (55 °C).

equilibrium is reached under low Cs loading condition. It has been reported that under diluted condition ($\leqq 10^{-7}$ M), the diffusion of adsorbed Cs ions on the external surface of minerals towards their internal sorption sites is accounted for the slower equilibrium [3,6,7]. However, the amount of these internal sorption sites is relatively few and hence it is difficult to observe the contribution from this factor on Cs adsorption under higher Cs loadings as shown in this work. More importantly, this diffusion is reduced under higher loadings because the rate of adsorbed ions transferring from the surface to internal sorption sites decreases as the loading increases [8].

At an elevated temperature, it takes more time to reach adsorption equilibrium. In other words, k value is higher at 25 °C than at 55 °C. It is due to the fact that these adsorbed Cs ions have higher energy (thermal energy) to escape from the granite surface. It is also noted that the difference between these two k values becomes insignificant as Cs loading decreases. This is related to the variety of sorption sites of granite surface. It will be further discussed in the following section.

We also compute the activation energy (E_a) of adsorption (kJ mol^{-1}) by comparing two rate constants determined under two temperatures using the equation:

$$\ln \frac{k_2}{k_1} = -\frac{E_a}{R}\left(\frac{1}{T_2} - \frac{1}{T_1}\right) \quad (2)$$

where R is the ideal gas constant (8.314 J mol^{-1}), k_1 and k_2 are rate constants under high and low temperatures. As shown in Table 2, the median value of E_a was 7.8 J mol^{-1}, suggesting that Cs adsorption is a physicosorption reaction, in which weak electrostatic force drives the ion-exchange reaction [8–12].

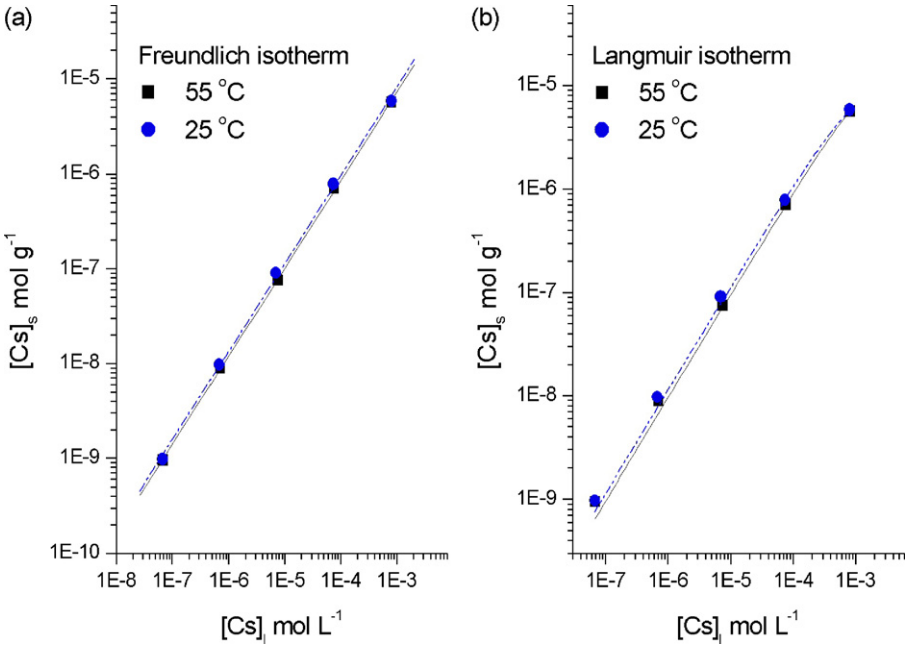

Fig. 2. Freundlich (a) and Langmuir isotherms (b) simulation at low (25 °C) and high temperature (55 °C).

3.2. Isotherms and thermodynamic parameters

The correlation between adsorbed Cs ions on solid surface and those remaining in solution is described by isotherm models. All experimental data were first fitted with Freundlich isotherm model. The concept of Freundlich model is based on multilayer adsorption associated with adsorption on heterogeneous surfaces [9] and its linear form is expressed as

$$\ln [Cs]_s = \ln k + 1/n \ln [Cs]_l \quad (3)$$

where the $[Cs]_s$ is the amount of Cs ions adsorbed on solid surface (mol g^{-1}) and was obtained using the following equation:

$$[Cs]_s = \frac{[Cs]_0 - [Cs]_l}{V/m} \quad (4)$$

$[Cs]_0$ is the initial Cs concentration (mol L^{-1}), V is the volume of the Cs solution (L) and m is the mass of the granite sample (g). The k value in Eq. (3) is the Freundlich constant and n is a constant related to the adsorption linearity. The magnitude of k value can be viewed as a rough indicator of adsorption affinity of granite samples towards the Cs ions [8,11,13]. As shown in Table 3, the reaction temperature has little effect on n value. Almost identical n values are observed under given reaction temperatures (n = 1.08). The fact that these two n values are very close to unity indicates that the effect of heterogeneous structure on the surface of adsorbents is not significant [8,10,11,13]. On the other hand, a relatively higher k value at low temperature demonstrates that granite has a decreasing affinity towards Cs ions with the increase of temperature. This can be attributed to the enhancement of Cs desorption at an elevated temperature.

Our experimental data were also fitted by the Langmuir isotherm model expressed as the following:

$$[Cs]_s = \frac{Q_m b [Cs]_l}{1 + b[Cs]_l} \quad (5)$$

where the Q_m represents maximum (saturated) sorption sites and b is the Langmuir constant.

Langmuir sorption model is the simplest physically plausible model based on three assumptions: (a) sorption cannot proceed beyond monolayer coverage; (b) all sorption sites are equivalent and the surface is uniform; (c) the ability of a molecule to be adsorbed at a given site is not affected by the occupation of the neighboring sites [9,14]. As shown in Table 3, the R^2 values are very close to unity, demonstrating the nice fitting of Langmuir model to these adsorption experiments. It is important to note that Q_m value decreases as temperature increases (80 μmol g^{-1} at 25 °C and 10 μmol g^{-1} at 55 °C), which is in agreement with the observations that the Cs adsorption is relatively lower under an elevated temperature.

We further calculate the thermodynamic parameters of Cs adsorption onto granite by considering results from both kinetic and isotherm fittings. According to the definition of the value a of Eq. (1), it can be regarded as the equilibrium concentration of Cs ions in solutions. Substituting the value a into Eq. (5), the amount of adsorbed Cs ions at equilibrium is thus determined. Following the sequence of Eqs. (6)–(9), the thermodynamic parameters of enthalpy, Gibbs energy and entropy of Cs adsorption are obtained

Table 2
The values of a, b and k obtained by the first-order kinetics simulation $[Cs]_l = a + b\,e^{-kt}$

Initial $[Cs]_l$	a (25 °C/55 °C)	b (25 °C/55 °C)	k (25 °C/55 °C)	R^2 (25 °C/55 °C)	E_a (kJ mol^{-1})
10^{-3} M	$8.1 \times 10^{-4}/8.1 \times 10^{-4}$	$1.9 \times 10^{-4}/1.9 \times 10^{-4}$	1.077/0.799	0.976/0.992	7.8
10^{-4} M	$7.0 \times 10^{-5}/8.0 \times 10^{-5}$	$3.0 \times 10^{-5}/2.0 \times 10^{-5}$	0.596/0.187	0.987/0.995	30.3
10^{-5} M	$7.0 \times 10^{-6}/7.5 \times 10^{-6}$	$3.0 \times 10^{-6}/2.5 \times 10^{-6}$	0.471/0.345	0.992/0.997	8.1
10^{-6} M	$6.8 \times 10^{-7}/7.2 \times 10^{-7}$	$3.2 \times 10^{-7}/2.8 \times 10^{-7}$	0.410/0.333	0.971/0.981	5.4
10^{-7} M	$6.7 \times 10^{-8}/6.9 \times 10^{-8}$	$3.3 \times 10^{-8}/3.1 \times 10^{-8}$	0.360/0.486	0.997/0.973	−7.8

Table 3
The values of k, n and R^2 obtained by the Freundlich isotherm and that of Q_0, b and R^2 by the Langmuir isotherm simulation for Cs adsorption

T (°C)	Freundlich isotherm			Langmuir isotherm		
	n	k (mmol g^{-1})	R^2	Q_0 (mmol g^{-1})	b (L mmol^{-1})	R^2
25	1.08 ± 0.004	4.98 ± 0.09	0.999	0.83 ± 0.00	10.47 ± 2.89	0.999
55	1.08 ± 0.006	4.37 ± 0.11	0.999	0.01 ± 0.00	0.83 ± 0.00	1.000

[8,10,11] and are summarized in Table 4.

$$K_d = \frac{[Cs]_s}{[Cs]_l} (L\,g^{-1}) \quad (6)$$

$$\Delta H^0 = R \ln \frac{K_d(T_2)}{K_d(T_1)} \frac{T_1 T_2}{T_2 - T_1} \ (kJ\,mol^{-1}) \quad (7)$$

$$\Delta G^0 = -RT \ln K_d \ (kJ\,mol^{-1}) \quad (8)$$

$$\Delta S^0 = \frac{\Delta H^0 - \Delta G^0}{T} \ (J\,mol^{-1}\,K^{-1}) \quad (9)$$

The negative value of enthalpy ($\Delta H^0 < 0$) around -10 kJ mol^{-1} reveals that Cs adsorption is exothermic. Hence the adsorption is favored under lower temperatures. The less negative enthalpy value (<-25 kJ mol^{-1}) strongly points to a physicosorption reaction, in which the weakly electrostatic force drives this ion-exchange reaction [9]. The negative Gibbs energy (with median value about -5.0 and -6.1 kJ mol^{-1} at low and high temperature) indicates a spontaneous adsorption reaction. The negative entropy was interpreted as the result of a stable arrangement of adsorbed Cs on granite surface [8,11]. Although the steady thermodynamic parameters are achieved only at the Cs loading less than 1.0×10^{-5} M, it is in agreement that Cs adsorption onto granite is exothermic, spontaneous and favorable at lower temperatures.

3.3. Effect of ionic strength

To clarify the effect of ionic strength on Cs adsorption, a series of batch experiments were carried out with competing cations of Na^+, K^+, Ca^{2+} and Mg^{2+} whose concentration range from 1×10^{-3} M to 1.0 M. These four cations are selected due to their abundance in nature water. In addition, synthetic groundwater and synthetic seawater were also utilized as the nature aquifer analogs. As shown in Fig. 3, it is noted that the Cs adsorption sharply decreases as the ionic strength increases. The Cs adsorption ratio in DW (no competing cations present), which is not plotted in Fig. 3 due to the logarithm scale, is about 23%. The presence of divalent cation, Ca^{2+} and Mg^{2+}, inhibits about half of the Cs adsorption. Also, a significant negative correlation between the increasing Na^+ concentration and Cs adsorption is clearly observed. Among these cations, the presence of K ion strongly constraints the Cs adsorption, especially when potassium concentration exceeds 0.01 M. This is in good agreement with other investigations that Cs adsorption is via cation-exchange reactions, in which cations with similar radius and hydration energy compete more effectively against Cs ions on the mineral surface [6]. Accordingly, it is recognized that in GW and SW solutions the reduction of Cs adsorption is mainly related to the presence of K ion (ionic radius of 138 pm in comparison with 167 pm of Cs ions, and similar hydration energy) [15]. While Ca^{2+} as well as Na^+ also affect the Cs adsorption to a certain extent, it is due to their high contents in GW and SW solutions.

Table 4
The values of ΔH, ΔG and ΔS calculated from Cs adsorption

Initial $[Cs]_0$	K_d (mL g^{-1}) (25 °C/55 °C)	ΔH (kJ mol^{-1})	ΔG (kJ mol^{-1}) (25 °C/55 °C)	ΔS (J mol^{-1} K^{-1}) (25 °C/55 °C)
10^{-3} M	7.1/7.1	4.1	−4.9/−4.5	0.03/0.03
10^{-4} M	11/7.6	−10	−6.0/−5.0	−0.01/−0.02
10^{-5} M	12/7.6	−12	−6.1/−5.0	−0.02/−0.02
10^{-6} M	12/7.6	−12	−6.2/−5.0	−0.02/−0.02
10^{-7} M	12/7.6	−12	−6.2/−5.0	−0.02/−0.02

3.4. SEM/EDS studying of Cs adsorption

Another parallel experiment without spiking radioactive Cs tracer was conducted for further studying the microscale distribution of adsorbed Cs ions on the granite surface. The crushed granite samples were collected by filtration and dried under reduced pressure at 55 °C for 2 days. By integrating the SEM/EDS images with mapping results, the distribution of adsorbed Cs ions on the surface of these samples is clearly visualized. It has been reported that the laminar minerals have excellent affinity toward Cs ions, such as kaolinite [8], illite [16,17], and some micaceous minerals [3,6,7]. In crushed granite samples, the micaceous mineral identified by XRD patterns is biotite. As shown in Fig. 4a, the appearance of biotite within SEM image was enlarged by 500 times. Although Cs ions will also be adsorbed in the surface of other minerals, i.e. quartz in the granite samples, this is not observed due to the limitation of the SEM/EDS mapping technique. The frayed edge sorption sites of biotite are particularly highlighted with red rectangle (Fig. 4a) and enlarged by 8000 times (Fig. 4b). It has been reported that these disrupted frayed edges are of particularly favorite environment for Cs adsorption [3,6,7]. As a result, further SEM/EDS mapping was focused on recording Cs signals within this specific regime. At the frayed edge, piles of debris and isolated fractures may be the result of weathering (Fig. 4b). As shown in Fig. 5, the appearance (Fig. 5a and b) associated with mapping images of Cs (Fig. 5c and d) and K (Fig. 5e and f) signals clearly point out the locations of these two elements on biotite surface. The Cs signals (bright spots, Fig. 5c

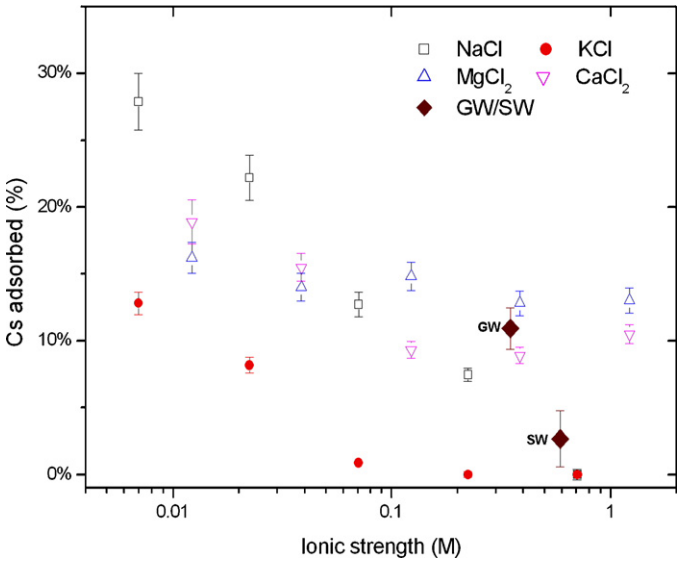

Fig. 3. Effect of ionic strength on Cs adsorption.

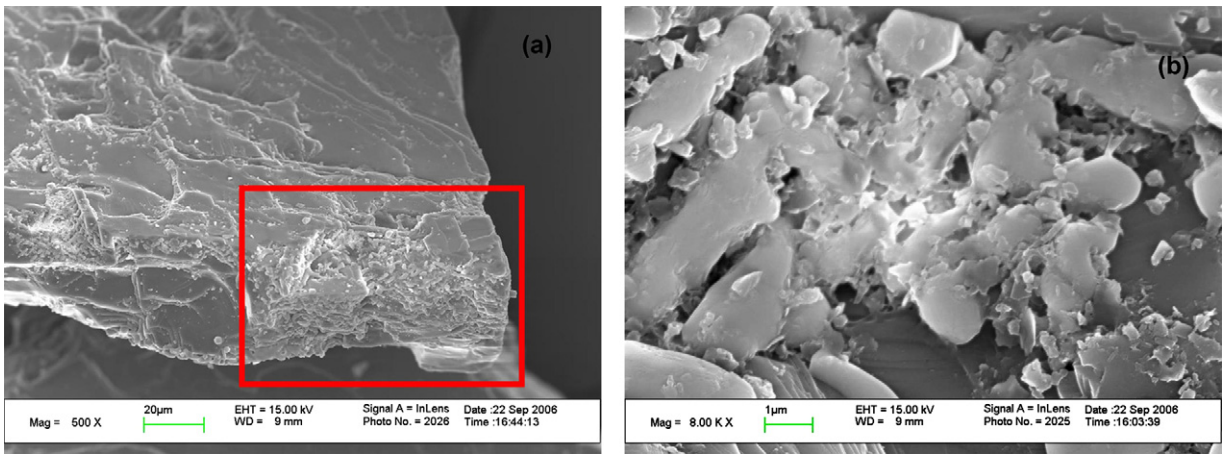

Fig. 4. A typical SEM image of macaceous minerals, biotite in this case, (a) 500× and (b) enlarging the area within red box by 8000×. (For interpretation of the references to color in this figure legend, the reader is referred to the web version of the article.)

and d) are particularly concentrated within the fractures and layer edges, the so-called frayed edges sorption sites (red arrows, Fig. 5a and b). In contrast, relatively fewer Cs signals are detected on the basal plane. This is due to the fact that the sorption sites of basal plane contribute little to Cs adsorption. In addition, it is significant that the bright-spot area of Cs signals is the counterpart of dark plateau of K signals, reflecting the depletion of potassium (Fig. 5e and f). The negative correlation between Cs and potassium is a typ-

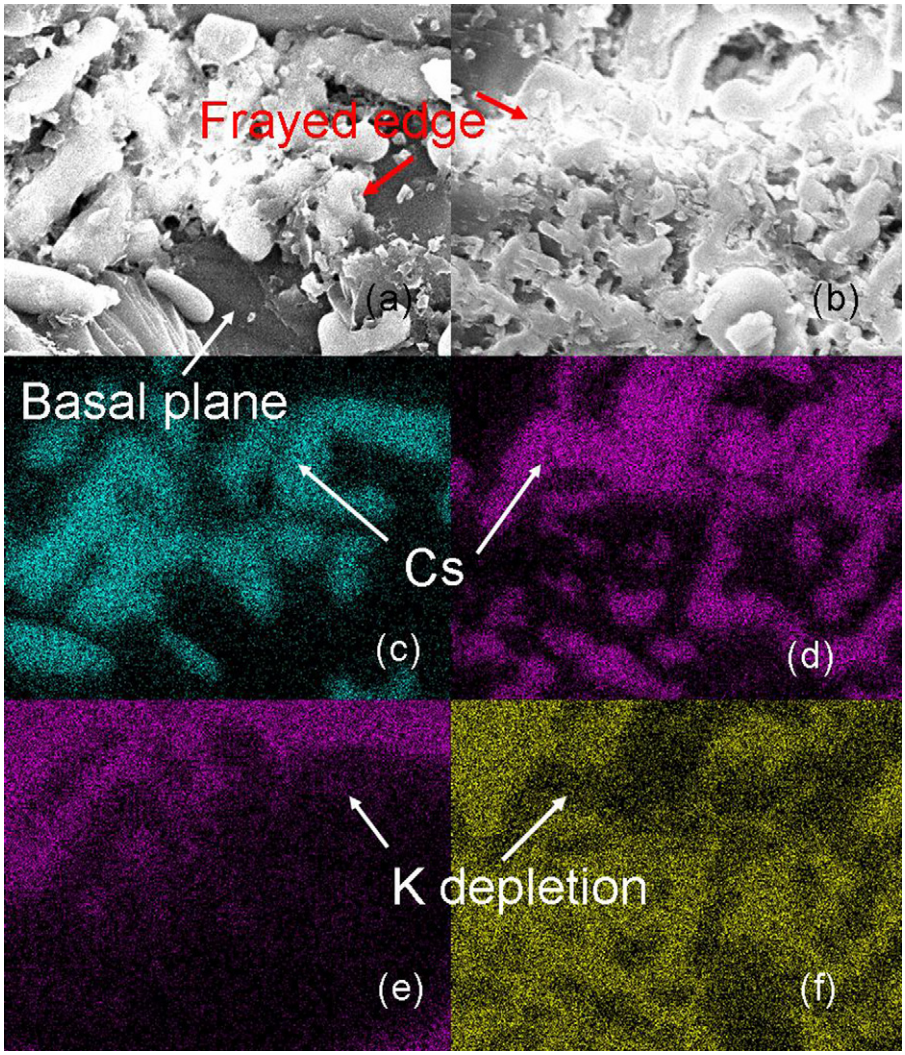

Fig. 5. SEM images of biotite surface being mapping (a and b), Cs signals (c and d), K signals (e and f), mapping area is 183 μm × 136 μm.

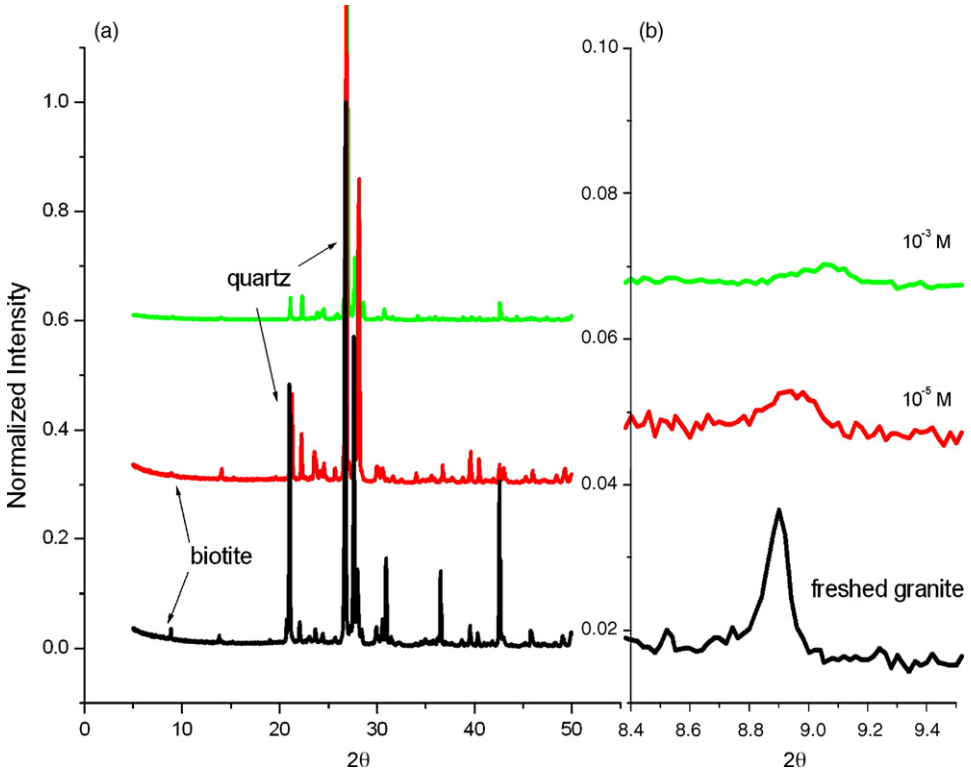

Fig. 6. XRD spectra of granite before and after Cs adsorption in normalized intensity. (a) The whole scanning angle; (b) enlarging the signals of biotite.

ical ion-exchange reaction, in which Cs replaces K at the frayed edge. Moreover, the bright plateau of K signals is in sharp contrast to the gloomy zone of Cs signals in the corresponding sites on the basal plane of biotite surface, implying a less Cs adsorption on this location [3,6,7].

The Fe (hydro)oxides have also been referred to as an important sorbent immobilizing Cs ions [3,12,18,19] though some crystalline Fe oxide has been synthesized for Cs adsorption [20]. However, in this work, no signals of Cs are detected even they were directly mapped onto the Fe oxides surface (i.e. goethite). This is in agreement with the observations that no significant relationship between Cs adsorption and Fe (hydro)oxides is proposed [1,21,22]. However, the probability of Cs adsorption onto iron oxides should not be completely ruled out based upon our EDS results because the detection limit of EDS is about 1% by weight.

3.5. XRD analysis of the Cs-adsorbed granite

XRD technique is utilized to examine the changes of micaceous minerals (biotite, in this work) by comparing the obtained XRD patterns before and after Cs adsorption. It has been reported that diffusion of adsorbed Cs from frayed edge site towards interlayer sorption sites will cause either swelling or collapse of the interlayer space. This phenomenon is frequently observed from the broadening and shifting signals within XRD pattern [3,6,7,23]. As shown in Fig. 6a, the normalized XRD patterns of granite before and after Cs adsorption seem to be identical. The d_{001} signal of biotite (indicated by black arrow) is enlarged in Fig. 6b. It is obvious that the normalized intensity of biotite signals becomes weak and shifted as the Cs loading increases. At the highest Cs loading (1×10^{-3} M), the biotite peak becomes blurred and faded into background signals. Although a substantial alteration in XRD patterns is observed, cautions should be taken to interpret this result since the intensity of biotite signals is quite low. Accordingly, a better explanation of XRD results is that biotite minerals dominate Cs adsorption onto granite and their interlayer spaces are greatly altered as the Cs loading increases. However, future work is required to investigate the magnitude of such interlayer alterations of biotite minerals. This should include further adsorption experiment with pure biotite minerals instead of the complex composition samples such as granite.

4. Conclusions

The Cs adsorption onto granite was conducted in deionized water to better understand its adsorption characteristics. Effects of factors including contact time, Cs loading and temperature on Cs adsorption were studied by a series of batch experiments. The kinetic adsorption was well simulated by a first-order kinetic equation. Both Freundlich and Langmuir sorption models were able to describe the Cs adsorption at given concentration (1×10^{-3} M to $\times 10^{-7}$ M) and the maximum sorption sites were 80 μmol g^{-1} at 25 °C and 10 μmol g^{-1} at 55 °C. The elevated temperature enhanced the desorption and thus produced a relatively lower adsorption. Generally speaking, the Cs adsorption onto granite was an exothermic ($\Delta H < 0$), spontaneous reaction ($\Delta G < 0$) and the forward reaction was favorable at low temperatures. Results of Cs adsorption under different ionic strength indicated that the presence of potassium remarkably reduces Cs adsorption. The mapping results clearly pointed out the adsorbed Cs is concentrated on the frayed edge of micaceous minerals at which potassium was depleted. In addition, XRD patterns showed the changes on biotite signals, indicating that biotite minerals are involved in Cs adsorption in granite. It is acknowledged that more experiments are required to investigate the magnitude of such changes of biotite minerals on Cs adsorption.

Acknowledgements

This work is supported by the Nuclear Backend Management Department at Taiwan Power Company, and the Energy and Resources Laboratories at Industrial Technology Research Institute (Taiwan).

References

[1] N. Marmier, A. Delisée, F. Fromage, Surface complexation modeling of Yb(III), Ni(II), and Cs(I) sorption on magnetite, J. Colloid Interface Sci. 211 (1997) 54–60.
[2] H.P. Cheng, M.H. Li, S. Li, A sensibility analysis of model selection in modeling the reactive transport of cesium in crushed granite, J. Contam. Hydrol. 61 (2003) 371–385.
[3] R.M. Cornell, Adsorption of cesium on minerals: a review, J. Radioanal. Nucl. Chem. 171 (1993) 483–500.
[4] T. Melkior, S. Yahiaoui, S. Motellier, D. Thoby, E. Tevissen, Cesium sorption and diffusion in Bure mudrock samples, Appl. Clay Sci. 29 (2005) 172–186.
[5] M.S. Murali, J.N. Mathur, Sorption characteristics of Am(III), Sr(II) and Cs(I) on bentonite and granite, J. Radioanal. Nucl. Chem. 254 (2002) 129–136.
[6] C.X. Liu, J.M. Zachara, S.C. Smith, J.P. Mckinley, C.C. Ainsworth, Desorption kinetics of radiocesium from subsurface sediments at Hanford Site, USA, Geochim. Cosmochim. Acta 67 (2003) 2893–2912.
[7] J.P. McKinley, J.M. Zachara, S.M. Heald, A. Dohnalkova, M.G. Newville, S.R. Sutton, Microscale distribution of cesium sorbed to biotite and muscovite, Environ. Sci. Technol. 38 (2004) 1017–1023.
[8] T. Shahwan, D. Akar, A.E. Eroglu, Physicochemical characterization of the retardation of aqueous Cs^+ ions by natural kaolinite and clinoptilolite minerals, J. Colloid Interface Sci. 285 (2005) 9–17.
[9] P.W. Atkins, Physical Chemistry, sixth ed., Oxford Press, New York, 1998.
[10] T. Shahwan, H.N. Erten, Thermodynamic parameters of Cs^+ on natural clays, J. Radioanal. Nucl. Chem. 253 (2002) 115–120.
[11] T. Shahwan, H.N. Erten, S. Unugur, A characterization study of some aspects of the adsorption of aqueous Co^{2+} on a natural bentonite clay, J. Colloid Interface Sci. 300 (2006) 447–452.
[12] J. Vejsada, E. Jelinek, Z. Randa, D. Hradil, R. Prikryl, Sorption of cesium on semectite-rich clays from the Bohemian Massif (Czech Republic) and their mixtures with sand, Appl. Radiat. Isot. 62 (2005) 91–96.
[13] S.P. Mishra, D. Tiwary, Ion exchangers in radioactive waste management VII: radiotracer studies on adsorption of Ba(II) and Sr(II) ions on hydrous thorium oxide, J. Radioanal. Nucl. Chem. 196 (1995) 353–361.
[14] G. Limousin, J.-P. Gaudet, L. Charlet, S. Szenknect, V. Barthes, M. Krimissa, Sorption isotherms: a review on physical bases, modeling and measurement, Appl. Geochem. 22 (2007) 247–279.
[15] G.L. Miessler, D.A. Tarr, Inorganic Chemistry, second ed., Prentice-Hall International, NJ, 1991.
[16] L. Bergaoui, J.F. Lambert, P. Prost, Cesium adsorption on soil clay: macroscopic and spectroscopic measurements, Appl. Clay Sci. 29 (2005) 23–29.
[17] B. Oztop, T. Shahwan, Modification of a montmorillonite-illite clay using alkaline hydrothermal treatment and its application for the removal of aqueous Cs^+ ions, J. Colloid Interface Sci. 295 (2006) 303–309.
[18] Y. Gossuin, J.-M. Colet, A. Roch, R.N. Muller, P. Gillis, Cesium adsorption in hydrated iron oxide particles suspensions: an NMR study, J. Magn. Reson. 157 (2002) 132–136.
[19] A. de Koning, A.V. Konoplev, R.N.J. Comans, Measuring the specific caesium sorption capacity of soils, sediments and clay minerals, Appl. Geochem. 22 (2007) 219–229.
[20] A. Dyer, M. Pillinger, J. Newton, R. Harjula, T. Möller, S. Amin, Sorption behavior of radionuclides on crystalline synthetic tunnel manganese oxides, Chem. Mater. 12 (2000) 3798–3804.
[21] C. Dumat, M.V. Cheshire, A.R. Fraser, C.A. Shand, S. Staunton, The effect of removal of soil organic matter and iron on the adsorption of radiocaesium, Eur. J. Soil Sci. 48 (1997) 675–683.
[22] F.G. Ferris, R.O. Hallberg, B. Lyvén, K. Pedersen, Retention of strontium, cesium, lead and uranium by bacterial iron oxides from a subterranean environment, Appl. Geochem. 15 (2000) 1035–1042.
[23] C.X. Liu, J.M. Zachara, S.C. Smith, A cation exchange model to describe Cs+ sorption at high ionic strength in subsurface sediments at Hanford site, USA, J. Contam. Hydro. 68 (2004) 217–238.